Magnetic Resonance Investigation of Vanadia and Vanadium−Molybdenum Gels Synthesized with Peroxovanadate Precursors

J. W. Wiench,[†] C. J. Fontenot,[†] J. F. Woodworth,[‡] G. L. Schrader,[†] M. Pruski,*[,†] and S. C. Larsen*[,‡]

Ames Laboratory (U.S. Department of Energy) and Department of Chemical Engineering, Iowa State University, Ames, Iowa 50011-3020, and Department of Chemistry, University of Iowa, Iowa City, Iowa 52242

Received: September 14, 2004; In Final Form: November 5, 2004

Vanadia gels and vanadium−molybdenum oxide gels were investigated using the magnetic resonance techniques, EPR spectroscopy and ^{51}V MAS NMR spectroscopy. The vanadium oxide gels were derived from the reaction of H_2O_2 and V_2O_5, and the vanadium−molybdenum oxide (VMoO) gels were derived from the reaction of peroxovanadates with an ammonium molybdate solution. EPR spectroscopy was utilized to determine quantitative information about the concentration of V^{4+} paramagnetic species present in the samples and additional structural information about the V^{4+} coordination environment. ^{51}V MAS NMR spectroscopy was used to elucidate the V^{5+} electronic environment and how it changes as a function of molybdenum content. The observed line broadening of the ^{51}V NMR signal with increasing molybdenum content was correlated with an increase in the concentration of paramagnetic species as monitored by EPR spectroscopy. The evolution of various vanadium sites during thermal treatment was also investigated. This work provides further support for the hypothesis that the selectivity of VMoO catalysts in the oxidation of 1,3-butadiene to maleic anhydride is due to the presence of paramagnetic V^{4+} sites.

1. Introduction

Vanadia gels have application as conductive coatings, electrochromatic films, cathode materials for lithium batteries,[1] and oxidation catalysts.[2,3] The gels can be prepared by various methods, including polymerization of decavanadic acid, dissolution of amorphous V_2O_5 in water, hydrolysis of alkoxides, and ion exchange of a $NaVO_3$ solution.[1] Recently, a sol−gel peroxovanadate route based on the reaction of H_2O_2 with V_2O_5 has been used to synthesize these materials.[4−6] The addition of molybdenum to these vanadia oxide gels by several different routes has been reported, along with limited characterization of the resulting VMoO materials.[3,7−9] The mixed-oxide materials have application as humidity sensors[7−9] and as catalysts for selective oxidation reactions.[2,3] Understanding the nature of the water coordination is important for both of these applications. The addition of water to the feedstock has been reported to increase both the selectivity and the activity of the VMoO catalyst in the oxidation of 1,3-butadiene.[2] Understanding the role of water incorporation is the first step in establishing the effect that water has on the surface reaction.

In our previous work, the peroxo-based $V_2O_5 \cdot nH_2O$ gels were extensively characterized by nuclear magnetic resonance (NMR) spectroscopy, X-ray diffraction (XRD), laser Raman spectroscopy, thermal gravimetric analysis (TGA), differential scanning calorimetry (DSC), and temperature-programmed desorption (TPD).[4−6] Solid-state NMR spectroscopy (^{51}V and ^{17}O) was our primary tool for characterization[4−6] because of the large chemical shift scale and strong dependence of NMR parameters on vanadium and oxygen coordination.[10,11] This extensive study revealed that the coordination of water played the largest role in the modification of the vanadia gel sites during dehydration. Five vanadium sites were described and quantified at various stages of hydration based on ^{51}V and ^{17}O NMR data.[5,6] However, although it is well-known that the diamagnetic V^{5+} oxidation state is the prevalent one in the vanadia gels, it is also known that paramagnetic V^{4+} is present in these materials. Electron paramagnetic resonance (EPR) spectroscopy can be used to obtain information about the concentration and coordination environment of V^{4+} sites in vanadia gels. Previously, EPR spectroscopy has been used to investigate the V^{4+} environment in related materials, such as amorphous V_2O_5 and vanadium phosphorus oxide (VPO) catalysts.[12,13]

In the work reported here, EPR spectroscopy and ^{51}V NMR spectroscopy are used to investigate the V^{4+} and V^{5+} sites, respectively, in vanadia and vanadium−molybdenum oxide gels. Taken together, these methods provide complementary information about the vanadium environments, the gelation process, and the role of water in these materials. The implications of these results with respect to the catalytic activity of the VMoO gels is also discussed.

2. Experimental Section

2.1. Sample Preparation. The vanadia gel sample was prepared with peroxovanadate precursors as described previously.[4,5] The VMoO samples were prepared by reacting an aqueous peroxovanadate solution with a molybdate solution at room temperature. The 0.26 M peroxovanadate solutions, which mostly consisted of the diperoxovanadium anion (small amounts of the monoperovanadium cation and the dimer), were prepared by reacting crystalline V_2O_5 (Asear) with 30% H_2O_2 (Fisher) using a H_2O_2/V_2O_5 molar ratio of 25. The molybdate solutions were prepared by dissolving diammonium molybdate in deionized water and were dried in air. Results are reported for four samples having 3.3, 14.0, 26.4, and 45.5 mol % MoO_3 in V_2O_5,

* To whom correspondence should be addressed. E-mail: Sarah-Larsen@uiowa.edu (S.C.L.); mpruski@iastate.edu (M.P.).
[†] Iowa State University.
[‡] University of Iowa.

10.1021/jp045848e CCC: $30.25
Published on Web 01/13/2005

which are referred to as samples A−D, respectively. The molar percent of MoO_3 in V_2O_5 was calculated as moles of MoO_3/(moles of MoO_3 + moles of V_2O_5) × 100% to facilitate comparison with the equilibrium phase diagram. As-synthesized samples B and D were also thermally treated at 100, 301, 324, and 403 °C prior to spectroscopic measurements. These samples, which are labeled as B100, B301, etc., were also analyzed using a Perkin-Elmer TGA 7 instrument at a heating rate of 5 °C/min in N_2.

2.2. Electron Paramagnetic Resonance (EPR) Spectroscopy. CW EPR (continuous-wave EPR) spectra were acquired using a Bruker EMX61 EPR spectrometer equipped with a PC for spectrometer control and data acquisition. A Bruker ER41111 variable-temperature unit with a temperature range from −163 to 400 °C was used to heat and cool the sample. Typical EPR spectral parameters were an X-band frequency of 9.43 GHz, a modulation amplitude of 0.5 G**,** and a modulation frequency of 100 kHz. The magnetic field and microwave frequency were measured using a Hall probe and a frequency counter, respectively. The signal intensity was calibrated with solutions of $VO(SO_4)\cdot nH_2O$, with $n = 3-5$ and $n_{TGA} = 4.7$, in water/glycerol with the concentration of V^{4+} species ranging from 1 to 21 wt %. EPR spectra were simulated using Bruker Simfonia software.

2.3. Solid-State NMR Spectroscopy. The solid-state NMR spectra of ^{51}V were obtained at room temperature using a Chemagnetics Infinity spectrometer operating at 9.4 T (105.17 MHz). Gels were dried at room temperature, placed in 3.2-mm rotors, and spun at 20 kHz in a Chemagnetics magic angle spinning (MAS) probe. Samples prepared in conjunction with thermal treatment were examined in the same manner following transfer of the sample to the probe within a glovebox under N_2.

MAS NMR spectra of ^{51}V were obtained using a Hahn echo sequence ($^1/_2\pi-\tau-\pi-\tau-$acquisition). Typically, 1000 scans were accumulated using a relaxation delay of 0.2 s. The NMR spectra exhibited superimposed, wide patterns of spinning sidebands, which were analyzed using the QUASAR simulation program, which used Herzfeld−Berger formalism.[14] All NMR shifts are reported using the δ scale, with positive values being downfield and referenced to $VOCl_3$.

3. Results and Discussion

3.1. EPR Spectroscopy of Vanadia Gels. The vanadia gels prepared with peroxovanadate precursors were pretreated ex situ at various temperatures, and the EPR spectra obtained at −163 °C are shown in Figure 1. The EPR spectrum of the vanadium gel before any thermal treatment (Figure 1a) is well-resolved and indicative of VO^{2+} ions in an axial crystal field. The EPR spectrum is dominated by the axial hyperfine interaction between the unpaired electron spin ($S = {}^1/_2$) and the ^{51}V nuclear spin ($I = {}^7/_2$, 99.8% natural abundance) and is characteristic of rigid-limit VO^{2+} systems (V^{4+}, d^1).[15] The EPR parameters obtained by spectral simulation of the spectrum in Figure 1a were $A_{||} =$ 546 MHz, $A_\perp = 209$ MHz, $g_{||} = 1.930$, and $g_\perp = 1.990$ and are listed in Table 1 along with the EPR parameters from the literature for related materials, such as amorphous V_2O_5 (hydrated and dehydrated), crystalline V_2O_5, and $[VO(H_2O)_5]^{2+}$.[15−17] The EPR parameters for amorphous V_2O_5 (hydrated) and $[VO(H_2O)_5]^{2+}$ are very similar to each other and to the EPR parameters of the fresh vanadia gel, suggesting an octahedral coordination environment for the VO^{2+} in the vanadia gel.

Slight changes in the EPR spectrum were observed when the fresh vanadia gel was exposed to dry nitrogen at room temperature for a period of 8−12 h, resulting in dehydration of the sample. The EPR parameters of this sample were obtained by spectral simulation and are also listed in Table 1. A decrease in the $A_{||}$ value (from 546 to 541 MHz) and a decrease in the $g_{||}$ value (from 1.930 to 1.915) were observed after the dry nitrogen treatment. A similar trend in EPR parameters was observed previously by Livage[16] and was attributed to the reversible hydration/dehydration of the vanadium center in amorphous V_2O_5 as illustrated by the EPR parameters listed in Table 1. The loss of a water ligand axial to the V═O bond is believed to be responsible for the observed change in the EPR parameters (decrease in $A_{||}$ and $g_{||}$).

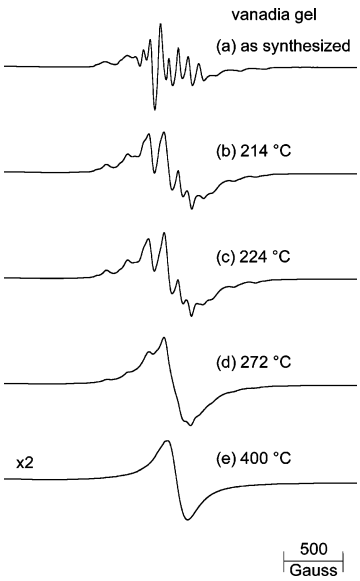

Figure 1. EPR spectra of a vanadia gel obtained at −163 °C after thermal treatments at the following temperatures: (a) room temperature, (b) 214, (c) 224, (d) 272, and (e) 400 °C. EPR spectra a−e were doubly integrated and after calibration with $VOSO_4$ standards, the following V^{4+} weight percentages were obtained: (a) room temperature, 1.2; (b) 214 °C, 1.9; (c) 224 °C, 1.9; (d) 272 °C, 1.9; (e) 400 °C, 1.2.

TABLE 1: EPR Parameters for Vanadia Gels and Related Materials[a]

	$g_{||}$	$g_\perp$	$A_{||}$ (MHz)	$A_\perp$ (MHz)	ref
amorphous V_2O_5					
dehydrated	1.913	1.98	493	185	16
hydrated	1.932	1.977	555	209	16
crystalline V_2O_5	1.915	1.987	NA	NA	17
$VO(H_2O)_5^{2+}$	1.933	1.978	547	212	15
vanadia gel (room temp)[a]	1.930	1.990	546	209	this work
vanadia gel (dry nitrogen)[a]	1.915	1.970	541	208	this work

[a] Estimated errors are ±0.001 for g and ±5 MHz for A.

As the vanadia gel is heated, spectral resolution decreases gradually until all of the hyperfine structure is gone and a completely exchange-narrowed EPR spectrum (Figure 1e) is observed after a gel thermal treatment temperature of 400 °C. The mechanism for exchange is a spin−spin exchange interaction between paramagnetic centers, possibly VO^{2+} dimers as suggested by previous ^{51}V MAS NMR studies.[4] Similar exchange-narrowed EPR spectra were observed in VPO catalyst materials.[12,13]

The EPR spectra in Figure 1 were also doubly integrated to obtain quantitative information about the concentrations of paramagnetic species. A calibration curve for standard $VOSO_4$ aqueous solutions was constructed so that the integrated areas could be converted into weight percentages of paramagnetic species in each sample. Assuming that the EPR signal is completely due to paramagnetic vanadium, the V^{4+} weight

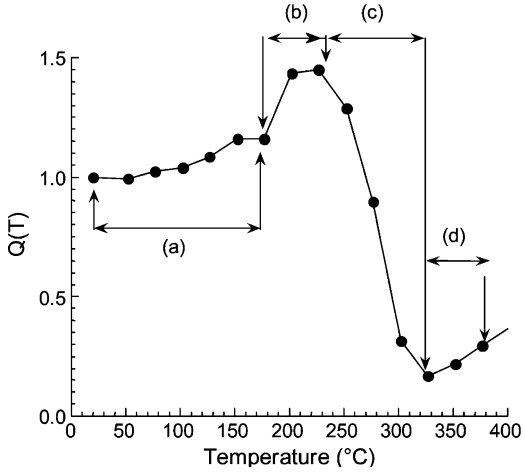

Figure 2. EPR signal intensity, Q(T), of the as-synthesized vanadia gel as a function of temperature. Several different regions are identified corresponding to (a) Curie−Weiss behavior; (b) transformation of V_3, V_4, and V_5 to V_1 and V_2; (c) transition state; (d) formation of ordered network.

percents obtained from the double integration of the EPR spectra in Figure 1a−e are 1.2%, 1.9%, 1.9%, 1.9%, and 1.2%, respectively. The V^{4+} weight percent values for the samples correspond to an average of approximately 3% of the total vanadium (V^{4+} and V^{5+}) that is present in these vanadia gels as V^{4+}. Because the concentration of paramagnetic species does not increase systematically as a function of pretreatment temperature, the exchange mechanism is hypothesized to be the result of a redistribution of the paramagnetic V^{4+} centers rather than an increase in concentration of V^{4+}.

To further understand the EPR spectra obtained after the various thermal treatments, a fresh vanadia gel sample was heated in situ, and EPR spectra were obtained at temperatures ranging from 25 to 400 °C. In previous EPR studies of VPO materials, spin exchange between paramagnetic V^{4+} centers was analyzed using the model function Q(T), where $Q(T) = TA(T)/T_RA(T_R)$.[12] A(T) is the integrated area of EPR spectrum at temperature T, and $A(T_R)$ is the integrated area at a reference temperature T_R. For pure paramagnetic (e.g., isolated V^{4+} centers) or Curie−Weiss behavior, Q(T) does not exhibit any temperature dependence.

The results of this analysis using Q(T) are plotted in Figure 2 using a reference temperature of 20 °C. In Figure 2, Curie Weiss behavior [Q(T) is independent of temperature] is observed from approximately 20 to 177 °C (region a). From approximately 177 to 227 °C (region b), an increase in spin exchange is observed, indicating an increase in structural order. Between 227 and 327 °C (region c), Q(T) drops off dramatically as the spin exchange collapses, indicating the formation of a disordered transition state. At above 327 °C (region d of Figure 2), the peak intensity begins to increase disproportionately, showing the return of spin exchange and the formation of an ordered, crystalline network.

3.2. Comparison with Previous NMR Results for Vanadia Gels. As mentioned in the Introduction, we recently reported the V^{5+} site coordinations along with the sites of water adsorption for a peroxo-based vanadia gel ($V_2O_5 \cdot nH_2O$).[5,6] Five vanadium sites (V_1-V_5) were identified using ^{51}V and ^{17}O solid-state NMR spectroscopy, including vanadium pentoxide (V_1, represented by a peak at around −620 ppm), vanadium pentoxide with a shifted layer below (V_2, at −597 ppm), vanadium dimer with one water molecule coordinated to each V site (V_3, at −664 ppm), vanadium oxide with one water molecule hydrogen-bonded to the vanadyl oxygen (V_4, at −593 ppm), and vanadium oxide with one water molecule coordinated trans to the vanadyl oxygen (V_5, at −572 ppm). Prior to dehydration, V_1 (18%), V_3 (5%), V_4 (45%), and V_5 (32%) species were present in the hydrated vanadia gels. As the dehydration progressed during thermal treatments, the concentration of water-free sites V_1 and V_2 increased at the expense of V_3, V_4, and V_5, reaching 69% and 31%, respectively, at 272 °C. Finally, the complete removal of water at 350 °C, the crystallization was complete, and only V_1 sites were detected.[5,6]

The EPR results reported here for the vanadia gels are consistent with the above ^{51}V NMR data. First, only a small percentage (∼3%) of the total vanadium is present as V^{4+} observed by EPR spectroscopy. This agrees well with previous results in the literature[18] and the estimates made in our ^{51}V NMR study, based on variable-temperature MAS experiments.[5] The coordination of the initial V^{4+} center in the hydrated vanadia gel is consistent with species with coordination environments depicted by V_1, V_3, V_4, and V_5 as found by a comparison of the EPR parameters with literature values for related complexes. The change in the EPR spectrum when the sample is treated at room temperature with dry nitrogen suggests that a weakly bound water is being lost as would be expected for species V_4 or V_5, where the water molecule is coordinated or hydrogen-bonded to the vanadyl oxygen. This process is reversible, as can be directly observed by EPR and NMR spectroscopies. An interesting result from the EPR data is the loss of resolution due to exchange narrowing that is observed as the thermal treatment temperature is increased. This indicates a redistribution of the V^{4+} centers so that they become close enough to interact with each other via a spin-exchange mechanism. This suggests that the V^{4+} centers are not evenly distributed through the vanadia gel as exchange interactions would not be expected to occur for a random distribution of V^{4+} centers at such a low concentration. Finally, the formation of an ordered network at above 327 °C (region d of Figure 2) is consistent with our earlier ^{51}V and ^{17}O NMR results, which detailed the presence of incommensurate interlayers in the hydrated vanadia gels and their disappearance at around 350 °C when the purely crystalline phase is formed.[5,6]

3.3. EPR Spectroscopy of VMoO Gels. The EPR spectra of VMoO gel samples B (14 mol % MoO_3) and D (46 mol % MoO_3) are shown in Figures 3 and 4, respectively, and the amounts of V^{4+} species are listed in Table 2. The samples were thermally treated ex situ at the indicated temperatures, and the EPR spectra were subsequently acquired at approximately −163 °C. Initially, the EPR spectrum of sample B (Figure 3a) has features similar to those of the EPR spectrum of the vanadia gel formed in the absence of molybdenum (Figure 1a). Indeed, the EPR parameters determined from the simulations of these two spectra are approximately the same and are indicative of VO^{2+} ions in an axial crystal field. The change in the EPR spectrum observed upon dehydration of sample B at room temperature (not shown) is also similar to that observed in the vanadia gel, suggesting the loss of an axial water ligand. Thus, the V^{4+} sites observed in the VMoO gel before any thermal treatments are similar to those in the vanadia gel without any molybdenum.

When the VMoO gel (sample B) is thermally treated, a gradual decrease in spectral resolution is observed, as can be seen in Figure 3b−e. An exchange-narrowed spectrum is observed at the highest thermal treatment temperatures. The amount of paramagnetic V^{4+} species in sample B increases from approximately 2 wt % in sample B to approximately 7 wt % in

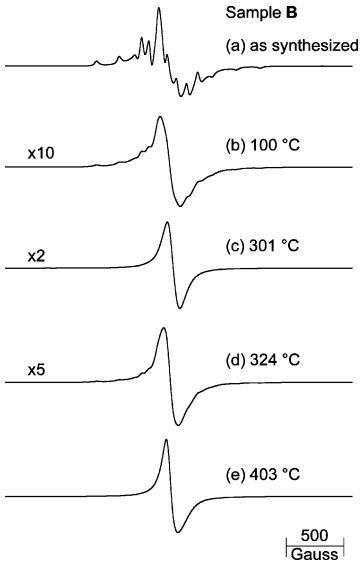

Figure 3. EPR spectra of a VMoO gel (sample B, 14 mol % MoO_3) obtained at −163 °C after thermal treatments: (a) B, (b) B100, (c) B301, (d) B324, and (e) B403. The EPR spectra a−e were doubly integrated, and after calibration with the $VOSO_4$ standard, the weight percentages reported in Table 2 were obtained. The sample masses in a−e are different, so spectral intensities are not directly comparable.

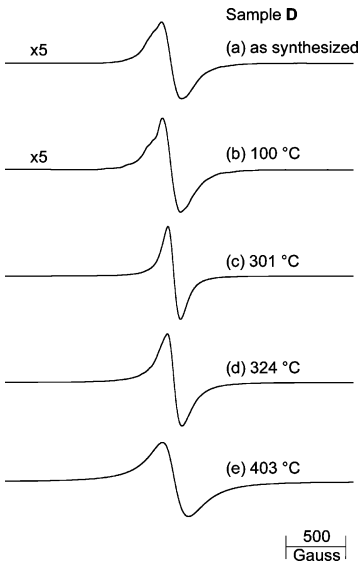

Figure 4. EPR spectra of a VMoO gel (sample D, 46 mol % MoO_3) obtained at −163 °C after thermal treatments: (a) D, (b) D100, (c) D301, (d) D324, and (e) D403. The EPR spectra a−e were doubly integrated, and after calibration with the $VOSO_4$ standard, the weight percentages reported in Table 2 were obtained. The sample masses in a−e are different, so spectral intensities are not directly comparable.

sample B403. This corresponds to a range of 4−14% of the total vanadium (V^{4+} + V^{5+}) that is present as V^{4+} (see Table 2).

The EPR spectra of VMoO gel (sample D) shown in Figure 4a-e are broad and unresolved prior to the thermal treatment. The weight percentage of V^{4+} increased from approximately 1% to 12% at progressively higher treatment temperatures, which corresponds to approximately 3−36% of the total vanadium being present as V^{4+} (see Table 2). These results are consistent with the NMR ^{51}V MAS spectra (vide infra), which show an increase in line broadening as the thermal treatment temperature of the VMoO gel is raised. Again, the EPR spectra

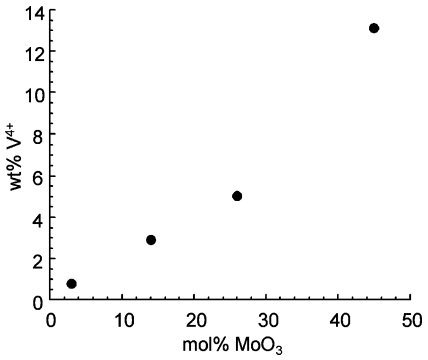

Figure 5. Graph of the weight percentage of V^{4+} paramagnetic species as a function of molybdenum content (mol % of MoO_3) for VMoO samples (A−D) after thermal treatment at 590 °C. The weight percentage of V^{4+} was obtained from analyis of the EPR spectra as described in the text.

TABLE 2: Amounts of Paramagnetic Species (V^{4+}) in Samples B and D Obtained from EPR Measurements[a]

sample	V^{4+} (wt %)	$V^{4+}/(V^{4+} + V^{5+})$ (%)
B	1.9	3.8
B100	4.0	8.1
B301	5.2	10.5
B324	4.4	8.4
B403	6.7	13.5
D	1.1	3.3
D100	1.9	5.6
D301	4.6	13.6
D324	6.1	18.0
D403	12.1	35.9

[a] Estimated error in V^{4+} weight percentage is ±1 wt %.

undergo exchange narrowing (Figure 4c) and then begin to broaden as the pretreatment temperature is further increased.

The exchange narrowing occurs via spin−spin exchange between paramagnetic centers. In contrast to the behavior of pure vanadia gels, the increase in spin−spin exchange can be explained by an increase in the paramagnetic V^{4+} concentration in the VMoO gels. The increase in concentration results in more V^{4+} centers that are close enough to interact via spin−spin exchange. In the case of the pure vanadia gels, the spin−spin exchange was attributed to a redistribution of V^{4+} sites because the overall paramagnetic intensity did not increase.

Samples with different molybdenum contents that had been thermally treated to the same temperature (590 °C) were also examined. The weight percent of paramagnetic V^{4+} species increased linearly with Mo content of the gel, as shown in Figure 5. This verifies the observed trend that the amount of paramagnetic vanadium produced in the VMoO gels increases with the Mo content.

Volkov and co-workers[19] proposed the following solid-state reaction for V_2O_5 and MoO_3 in which the vanadium is reduced from V^{5+} to V^{4+} during the reaction

$$V_2O_5 + ye^- \rightarrow V_2O_{5-y} + yO^-$$

$$(V_{1-x}Mo_x)_2O_{5+y} + ze^- \rightarrow (V_{1-x}Mo_x)_2O_{5+y-z} + zO^-$$

The increase in the V^{4+} concentration with Mo content and the temperature of thermal treatment observed in our study are consistent with this reaction.

3.4. Solid-State NMR Spectroscopy of VMoO Gels. ^{51}V MAS NMR spectra of as-synthesized samples are shown in Figure 6, and the spectra of thermally treated samples B and D

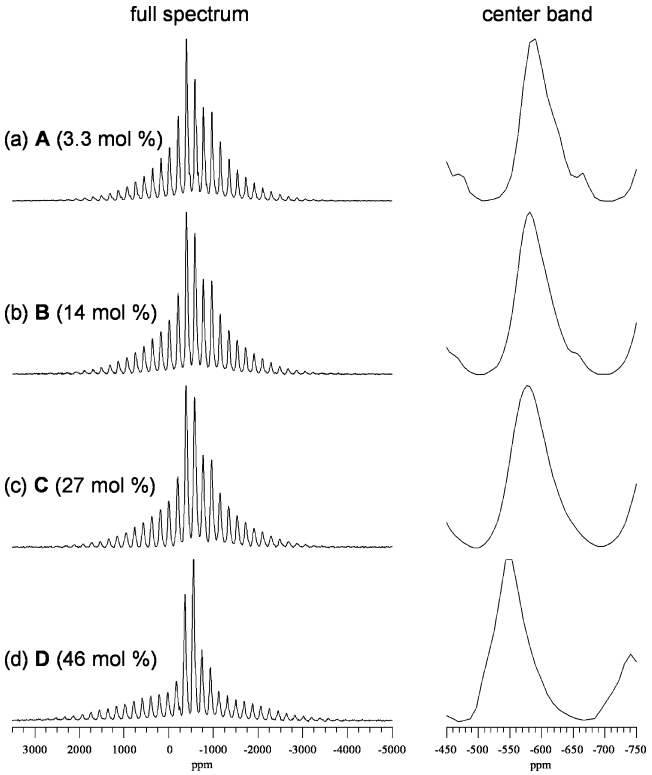

Figure 6. Full ^{51}V MAS NMR spectra (left side) and expanded isotropic area (right side) of as-synthesized VMoO gels for samples (a) A, (b) B, (c) C, and (d) D.

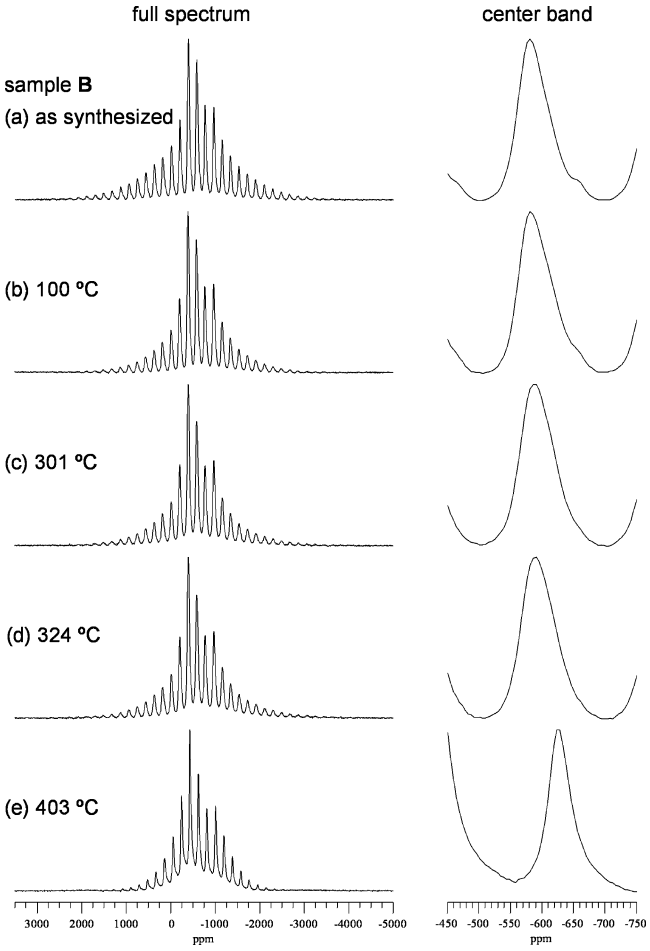

Figure 7. Full ^{51}V MAS NMR spectra (left side) and expanded isotropic area (right side) of a VMoO gel (sample B, 14 mol % MoO_3): (a) B, as-synthesized; (b) B100; (c) B301; (d) B324, and (e) B403.

are presented in Figures 7 and 8, respectively. The numerical simulations of these spectra, performed using the QUASAR program, included the effects of the chemical shift anisotropy (CSA) as well as first- and second-order quadrupolar interactions, as detailed in our earlier publications.[5,6] Several parameters describing these interactions in VMoO gels have been determined, including the quadrupole coupling constant (C_Q), the asymmetry parameter (η_Q), the isotropic chemical shift (δ_{ISO}), the CSA ($\Delta\delta_{CSA}$), and the CSA asymmetry parameter (η_{CSA}). These parameters, listed in Table 3, indicated that similar sites were present in most of the spectra. The relative concentrations of these sites are reported in Table 4.

We first note that the resolution observed in VMoO samples is lower than that observed in pure vanadia gels,[5,6] which is attributed to their less ordered structure and the increasing concentration of paramagnetic V^{4+} sites detected by EPR spectroscopy, especially in samples with higher Mo contents and/or higher temperatures of treatment. The spectra consist of several superimposed patterns of spinning sidebands that would be difficult to analyze without prior knowledge from the studies of pure vanadia gels.[5,6] By means of a strategy similar to that described in ref 5, we first simulated the spectra of sample A, using the results obtained for pure vanadia as the starting parameters. Other spectra were subsequently analyzed by varying the relative intensities, line broadening, and other parameters when needed. To fit the spectra of sample D, a new peak was introduced, which was assigned to V_2Mo. The principal components of the CSA tensors and the Euler angles between the CSA and quadrupolar tensors are not included in Table 3, because they were too unreliable to bear any important effect on the conclusions of this work. The important general observations are discussed below.

The center band for all sideband patterns was positioned near -600 ± 60 ppm, and $\Delta\delta_{CSA}$ was approximately -1000 ppm, which is characteristic of octahedral vanadates.[10] The resonances at -615 and -660 ppm, which were described as V_1 and V_3 in pure vanadia,[5,6] were present in all samples. The distinction between sites V_2, V_4, and V_5 could not be made during numerical analysis; therefore, these three sites were treated jointly as a single resonance at -580 ppm and denoted as V_x. The numerical simulations showed that δ_{CSA} varied from -710 to -1080 and η_{CSA} varied from 0.4 to 0.7 for this site, which might be due to varying contributions of V_2, V_4, and V_5 sites at different temperatures. We could not confirm the presence of site(s) V_x at the highest Mo concentration (sample D). Instead, a new resonance at -550 ppm became dominant, which we denoted as V_2Mo (see section 3.5).

Table 4 shows that the relative concentrations of sites V_1, V_2, and V_x remained relatively unaffected by the presence of low concentration of Mo and the thermal treatment up to 324 °C. A major increase of the V_1 concentration was observed at temperatures above 400 °C, where the crystalline V_2O_5 begins to form. We note that, in pure vanadia gels, the crystallization took place at lower temperatures, as evidenced by the corresponding increase in V_1 concentration. Specifically, the amount of V_1 sites in the vanadium oxide gel doubled when the temperature of thermal treatment was increased from 224 to 272 °C.[3,5]

3.5. Structural Interpretation of the Magnetic Resonance Results for VMoO Gels. For sample A, the NMR and EPR results are similar to those for a pure $V_2O_5 \cdot nH_2O$ gel, which indicates that, at low concentrations of molybdenum, the VMoO gel forms a layered structure similar to that existing in the

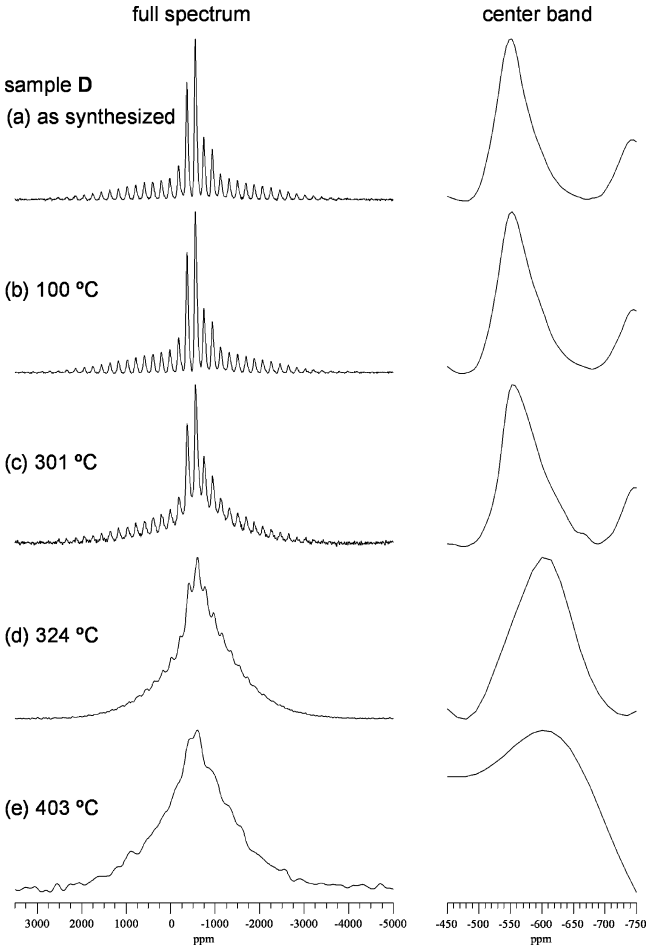

Figure 8. Full ^{51}V MAS NMR spectra (left side) and expanded isotropic area (right side) of a VMoO gel (sample D, 46 mol % MoO_3): (a) D, (b) D100, (c) D301, (d) D324, and (e) D403.

TABLE 3: Line Shape Parameters δ_{ISO} (ppm), C_Q (MHz), η_Q, $\Delta\delta_{CSA}$ (ppm), and η_{CSA} of Vanadium Sites in VMoO Gels Obtained by Numerical Simulations of ^{51}V MAS NMR Spectra[a]

site	δ_{ISO}	C_Q	η_Q	$\Delta\delta_{CSA}$	η_{CSA}
V_1	−615	1.4	0.8	−750	0.5
V_3	−660	0.7	0.7	−970	0.6
V_x	−580	1.6	0.6	−710 to −1080	0.4−0.7
V_2Mo	−550	0.6	0.6	−970	0.6

[a] Chemical shift anisotropy (CSA) tensor parameters are related to the components of the CSA tensor δ_{ii} as follows: $\delta_{ISO} = (\delta_{11} + \delta_{22} + \delta_{33})/3$, $\Delta\delta_{CSA} = {}^3/_2(\delta_{33} - \delta_{iso})$, and $\eta_{CSA} = (\delta_{22} - \delta_{11})/(\delta_{33} - \delta_{ISO})$, assuming $|\delta_{33} - \delta_{ISO}| \geq |\delta_{11} - \delta_{ISO}| \geq |\delta_{22} - \delta_{ISO}|$. The data were obtained with the following accuracies: δ_{ISO}, ±5 ppm; C_Q, ±0.1 MHz; η_Q and η_{CSA}, ±0.1; $\Delta\delta_{CSA}$, ±70 ppm.

TABLE 4: Relative Concentrations[a] of Vanadium Sites in the VMoO Gels Studied

site	A	B	B100	B301	B324	B403	C	D	D100	D301
V_1	16	11	11	11	10	84	12	11	17	18
V_3	4	3	6	6	7	16	1	2	3	3
V_x	80	86	84	84	83		84			
V_2Mo								87	80	79

[a] Error is ±2% except for sample B403 (±3%).

absence of molybdenum.[5,6] The ^{51}V NMR spectra of as-synthesized samples B and C are also similar in the sense that the V_1, V_3, and V_x environments are present in equivalent amounts (Figure 6a−c and Table 4). Thus, although the molar ratio of V to Mo decreases from almost 60:1 for sample A to 5.6:1 for sample C, these materials seem to undergo severe structural changes. The NMR spectrum of as-synthesized sample D also includes resonances representing V_1 and V_3. As mentioned earlier, it is dominated by a previously undetected peak at −550 ppm (site V_2Mo). Indeed, the numerical analysis of ^{51}V NMR spectra revealed that the peak at −550 ppm represents an octahedrally coordinated vanadium site, which we assign to V_2MoO_8 phase. First, the molecular formula for sample D is $V_{2.4}MoO_9$, which is close to V_2MoO_8 phase found previously in V_2O_5·MoO_3 systems.[20] Second, the crystal structure of V_2MoO_8 is known to be closely related to V_2O_5 and includes octahedrally coordinated vanadium.[21] The observed 30 ppm downfield shift of the V_2Mo site resonance with respect to V_x site(s) can be attributed to the deshielding effect caused by substituting two V atoms by Mo atoms.

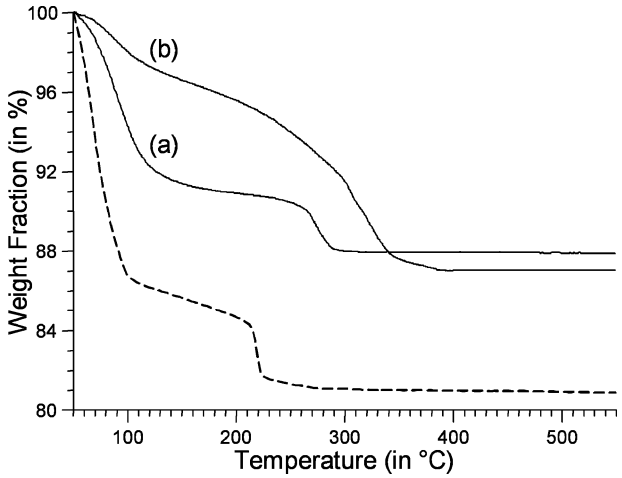

Figure 9. TGA curves recorded for samples (a) B and (b) D in comparison with the curve for the layered vanadia gel (dashed line) from ref 5.

Despite the lower resolution of ^{51}V NMR spectra, much can still be learned from the ^{51}V NMR characterization of thermally treated VMoO samples. First, because the addition of molybdenum oxide affected the ^{51}V MAS NMR spectra uniformly, the VMoO gels behave as homogeneous solid solutions of V_2O_5 and MoO_3 at all compositions studied. Second, the dehydration of VMoO gels occurs at considerably higher temperatures than in pure vanadia, especially at the highest Mo content. This was observed by NMR spectroscopy in sample B403 and in the TGA curves of all samples (examples of such curves are shown in Figure 9). Third, at temperatures up to 324 °C, the concentration of V_x sites in VMoO is approximately equal to the combined concentration of sites V_2, V_4, and V_5 found in V_2O_5 gels (up to 215 °C). In this temperature range, the analysis of $\Delta\delta_{CSA}$ and η_{CSA} for the V_x resonance was irrelevant, because each of the unresolved sites V_2, V_4, and V_5 that contributed significantly to V_x has different values of these parameters.[5,6] However, at temperatures above 300 °C, the line shape parameters were consistent with the increased relative contribution of V_2 sites, which further suggests that the VMoO gels form a layered structure.

In contrast to the V_2O_5·nH_2O gel sample, the V_3 site is present in all spectra of samples B and D regardless of the temperature of thermal treatment. This can be explained if we assume that this site is a connecting point between shear planes as found in V_2MoO_8 phase.[21] That would further imply that such shear planes exist in the vanadium−molybdenum phase and are stabilized by the presence of molybdenum octahedra.

3.6. Implications for Catalysis. In previous catalytic studies of 1,3-butadiene oxidation on VMoO materials, the catalyst with

the highest concentration of molybdenum exhibited the best selectivity to maleic anhydride.[2] This increase in selectivity was attributed to the presence of nucleophilic oxygen associated with $V^{4+}-O$ sites. The results reported here indicate that the concentration of paramagnetic V^{4+} as monitored by EPR spectroscopy does increase linearly with molybdenum concentration in the VMoO gels. This provides further support for the hypothesis that the selectivity is due to the presence of paramagnetic V^{4+} sites.

Addition of a small amount of water (2.5%) to a feedstock during 1,3-butadiene oxidation increased both the conversion rate and the selectivity to crotonaldehyde and furane.[2] The presence of water in the structure of the VMoO gels supports the previously proposed explanation that water molecules accelerate the desorption of products from the catalyst surface.[2] The calcination temperature of the gels might also be an important parameter in preserving the structure of the VMoO gels.

4. Conclusions

Using ^{51}V MAS NMR and EPR spectroscopies, V^{4+} and V^{5+} sites in vanadia gels and vanadium−molybdenum oxide gels were investigated. The vanadia gels exhibited low concentrations of paramagnetic V^{4+} (3% of total vanadium was present as V^{4+}) in agreement with previous ^{51}V MAS NMR results. The EPR spectra of the VMoO gels indicated the presence of increasing amounts of paramagnetic V^{4+} with increasing pretreatment temperature (for a constant Mo concentration) and with increasing Mo concentration (for a constant pretreatment temperature). The EPR results correlated well with the ^{51}V MAS NMR spectra for the VMoO gels in which broadening was observed concomitant with the observed increase in EPR signal intensity. Despite the lower resolution of ^{51}V NMR spectra due to the paramagnetic broadening, the ^{51}V NMR spectra provided structural information about the thermally treated VMoO samples. The addition of molybdenum oxide affected the ^{51}V MAS NMR spectra uniformly, suggesting that the VMoO gels behaved as homogeneous solid solutions of V_2O_5 and MoO_3 at all compositions studied. Vanadium sites in the VMoO gels were identified, quantified, and compared with vanadium sites observed in vanadia gels. The increase in V^{4+} concentration (as measured by EPR spectroscopy) with increasing molybdenum content in the VMoO gels correlated well with the previously observed increase in the selectivity of VMoO catalysts in the oxidation of 1,3-butadiene to maleic anhydride. This supports the hypothesis that the V^{4+} sites are responsible for the selectivity in this reaction.

Acknowledgment. This research was supported at Ames Laboratory by the U.S. Department of Energy, Office of Basic Energy Sciences, Division of Chemical Sciences, under Contract W-7405-Eng-82 and by the NSF (CHE0204847 to S.C.L.).

References and Notes

(1) Watanabe, T.; Ikeda, Y.; Ono, T.; Hibino, M.; Hosoda, M.; Sakai, K.; Kudo, T. *Solid State Ionics* **2002**, *151*, 313−320.
(2) Schroeder, W. D.; Fontenot, C. J.; Schrader, G. L. *J. Catal.* **2001**, *203*, 382−392.
(3) Franca, M. C. K.; San Gil, R. A. D. S.; Eon, J.-G. *Catal. Today* **2003**, *78*, 105−115.
(4) Fontenot, C. J.; Wiench, J. W.; Pruski, M.; Schrader, G. L. *J. Phys. Chem. B* **2000**, *104*, 11622−11631.
(5) Fontenot, C. J.; Wiench, J. W.; Pruski, M.; Schrader, G. L. *J. Phys. Chem. B* **2001**, *105*, 10496−10504.
(6) Fontenot, C. J.; Wiench, J. W.; Schrader, G. L.; Pruski, M. *J. Am. Chem. Soc.* **2002**, *124*, 8435−8444.
(7) Bondarenka, V.; Grebinskij, S.; Mickevicius, S.; Volkov, V.; Zacharova, G. *J. Non-Cryst. Solids* **1998**, *226*, 1−10.
(8) Tong, M.; Dai, G.; Wu, Y.; He, X.; Yan, W.; Gao, D.; Volkow, V.; Zakharova, G. *J. Mater. Res.* **2000**, *15*, 2653−2657.
(9) Harreld, J.; Dong, W.; Dunn, B. *Mater. Res. Bull.* **1998**, *33*, 561−567.
(10) Mastikhin, V. M.; Lapina, O. B. In *Encyclopedia of Nuclear Magnetic Resonance*; Grand, D. M., Harris, R. K., Eds.; John Wiley & Sons: Chichester, U.K., 1996; Vol. 8, pp 4892−4904.
(11) Lapina, O. B.; Shubin, A. A.; Khabibulin, D. F.; Terskikh, V. V.; Bodart, P. R.; Amoureux, J. P. *Catal. Today* **2003**, *78*, 91−104.
(12) Bruckner, A.; Kubias, B.; Lucke, B. *Catal. Today* **1996**, *32*, 215−222.
(13) Bruckner, A.; Martin, A.; Kubias, B.; Lucke, B. *J. Chem Soc., Faraday Trans.* **1998**, *94*, 2221−2225.
(14) Herzfeld, J.; Berger, A. E. *J. Chem. Phys.* **1980**, *73*, 6021.
(15) Chasteen, N. D. In *Biological Magnetic Resonance*; Reuben, J., Ed.; Plenum Press: New York, 1981; Vol. 3, p 53.
(16) Nabavi, M.; Sanchez, C.; Livage, J. *Philos. Mag. B* **1991**, *63*, 941−953.
(17) Gillis, E.; Boesman, E. *Phys. Status Solidi* **1966**, *14*, 337−353.
(18) Pozarnsky, G. A.; McCormick, A. V. *Chem. Mater.* **1994**, *6*, 380−385.
(19) Volkov, V. L. *Russ. J. Phys. Chem.* **1985**, *59*, 247.
(20) Magneli, A.; Blomberg, B. *Acta Chem. Scand.* **1951**, *5*, 585−589.
(21) Eick, H. A.; Kihlborg, L. *Acta Chem. Scand.* **1966**, *20*, 1658−1666.